Volume 24, No 4 | International Journal of Radiation Research, October 2026

Risk prediction model of radiation encephalopathy based on MRI white matter high signal load

H. Ge, Y. Zhang, G. Tong*

Department of Radiation Oncology, The Affiliated Hospital, Medical University, China

► ***Original article***

***Corresponding author:**
Guoqin Tong, M.D.,
E-mail:
tongguoqin@hospital.edu.cn

Received: September 2025
Final revised: August 2026
Accepted: August 2026

Int. J. Radiat. Res., October 2026; 24(4): 1165-1173

DOI: 10.61186/ijrr.24.4.30

Keywords: *Magnetic resonance imaging, white matter hyperintensities, radiation injuries, apolipoprotein e4, dose-response relationship, radiation, head and neck neoplasms.*

ABSTRACT

Background: A prediction model of Radiation Encephalopathy (RE) based on White Matter Hyperintensity (WMH) load of Magnetic Resonance Imaging (MRI) was constructed. ***Materials and Methods:*** One hundred and fifty-three patients with head and neck malignant tumor (nasopharyngeal carcinoma, intracranial tumor) who received radiotherapy were retrospectively included and divided into RE group (n=17) and non-RE group (n=136). E(Apolipoprotein E (APOE)ε4 gene expression was detected, and radiotherapy dose, Fazekas score, V_{30} and maximum dose (D_{max}) were collected. Logistic regression was used to screen the risk factors, and ROC curve was used to evaluate the predictive efficacy. ***Results:*** APOE ε4 carriers, radiotherapy dose, Fazekas score, V_{30} and D_{max} were independent risk factors for RE ($P<0.05$). The area under the curve (AUC) of the joint prediction model is 0.921, and the prediction efficiency is better than that of a single index. ***Conclusion:*** The model based on MRI-WMH load combined with radiation dosimetry parameters has high prediction accuracy, which can screen the high-risk population of RE at an early stage and provide reference for clinical individualized radiotherapy.

INTRODUCTION

Radiotherapy techniques for head and neck malignancies have become increasingly sophisticated, significantly prolonging patient survival. However, radiation encephalopathy (RE), an irreversible delayed neurological complication following radiotherapy, exhibits a rising incidence year by year. Its clinical manifestations include cognitive decline and motor dysfunction, severely impairing patients' quality of life [1, 2]. RE develops insidiously, with no specific early clinical symptoms, and conventional imaging modalities often fail to detect early brain tissue damage. Most patients are diagnosed only after irreversible neurodegeneration has occurred, leaving limited effective intervention options [3]. White Matter Hyperintensity (WMH), a characteristic abnormal bright signal on MRI FLAIR sequences, quantitatively reflects cerebral microvascular injury and the extent of white matter demyelination, serving as a critical imaging biomarker for assessing brain radiation tolerance [4]. The Apolipoprotein E (APOE) gene is pivotal for lipid transport in the central nervous system, with the APOE ε4 subtype identified as a genetic susceptibility factor for radiation-induced neurological damage. APOE ε4 disrupts blood-brain barrier integrity, exacerbates neuroinflammatory responses, and amplifies the damaging effects of ionizing radiation on brain tissue, markedly increasing the risk of RE onset [5]. Current domestic and international research on radiation-induced leukoencephalopathy (RE) prediction primarily focuses solely on radiotherapy dose parameters, with few studies integrating genetic susceptibility factors and preoperative white matter hyperintensity (WMH) imaging load. Moreover, there is a lack of a unified and streamlined clinical prediction model [6]. Existing studies still suffer from excessive confounding factors, redundant screening indicators, and poor clinical applicability of the models. Therefore, this study focuses on three core objective indicators: imaging data, genetic factors, and radiotherapy dose. For the first time, it combines MRI WMH load, APOE ε4 gene polymorphism, and dose-volume histogram parameters to construct a RE prediction model. The study elucidates the patterns of pre-and post-radiotherapy white matter imaging changes and quantifies the threshold values for multi-index combined prediction, providing a standardized tool for non-invasive, early, and convenient clinical screening of high-risk populations for RE.

Recent epidemiological studies have demonstrated that the incidence of radiation-induced brain injury ranges from 5% to 50% depending on radiation dose, volume, and individual susceptibility, with nasopharyngeal carcinoma patients being particularly vulnerable due to the proximity of the temporal lobes to the radiation field [7, 8]. A prospective study by Hsiao *et al*. reported cognitive deterioration following intensity-modulated

[Downloaded from ijrr.com on 2026-11-23]

[DOI: 10.61186/ijrr.24.4.30]

radiation therapy (IMRT) in patients with nasopharyngeal carcinoma [9]. White matter hyperintensity (WMH), initially described in the context of cerebral small vessel disease, has emerged as a sensitive imaging biomarker of subclinical brain injury. The Fazekas visual rating scale, introduced in 1987, remains the most widely used method for quantifying WMH burden in clinical practice and research [10]. Multiple cross-sectional studies have demonstrated that higher baseline Fazekas scores are associated with increased risk of post-radiotherapy cognitive deterioration, suggesting that pre-existing microvascular pathology may lower the threshold for radiation-induced white matter damage [11, 12]. From a genetic perspective, the apolipoprotein E (APOE) gene, located on chromosome 19q13.2, encodes a major cholesterol transport protein in the central nervous system. The APOE ε4 allele, carried by approximately 15-20% of the general population, has been consistently associated with increased risk of Alzheimer's disease and poor outcomes after traumatic brain injury [13, 14]. In the context of radiation oncology, emerging evidence suggests that APOE ε4 carriers exhibit enhanced blood-brain barrier disruption and neuroinflammatory responses following cranial irradiation, although the exact molecular mechanisms remain incompletely elucidated [15, 16]. Dosimetric parameters, particularly V_{30} (volume receiving ≥30 Gy) and D_{max} (maximum point dose), have been identified as critical predictors of radiation necrosis in multiple organs at risk. Su *et al*. evaluated dose-volume parameters associated with temporal lobe necrosis following intensity-modulated radiotherapy in patients with nasopharyngeal carcinoma [17]. However, most existing prediction models rely exclusively on dosimetric parameters and fail to incorporate individual biological susceptibility factors, limiting their predictive accuracy and clinical utility [18].

The novelty of this study lies in three aspects: (1) For the first time, we integrate three complementary dimensions - MRI-based white matter hyperintensity load (imaging phenotype), APOE ε4 genetic polymorphism (biological susceptibility), and dose-volume histogram parameters (physical exposure) - into a unified prediction model for radiation encephalopathy, moving beyond conventional single-modality approaches. (2) We establish quantitative threshold values for multi-index combined prediction, providing clinicians with an actionable, standardized tool for early risk stratification. (3) We systematically characterize the temporal patterns of white matter imaging changes before and after radiotherapy, offering insights into the dynamic progression of radiation-induced white matter injury that may inform timely intervention strategies.

MATERIALS AND METHODS

General information

A retrospective study was conducted involving 153 patients with nasopharyngeal carcinoma or intracranial tumors who received radiotherapy at our hospital from January 2021 to June 2025. These patients were classified into the radiation-induced encephalopathy (RE) group (n=17) and the non-RE group (n=136) based on the occurrence of RE post-radiotherapy. Non-objective confounding factors such as BMI, hypertension, diabetes, place of residence, and smoking/alcohol consumption history were excluded; only imaging data, genetic information, and radiotherapy dose-related data were retained. The study was approved by the Medical Ethics Committee (Approval No.: KY-2025-0612; Approval Date: June 8, 2025). All patients provided informed consent, and the study strictly adhered to the Helsinki Declaration.

***Inclusion criteria*:** (1) Adults with head and neck malignancies (e.g., nasopharyngeal carcinoma, brain tumors) receiving initial radical radiotherapy; (2) Radiotherapy completion time ≥6 months (excluding acute-phase reactions); (3) Baseline MRI showing white matter hyperintensity (WMH) prior to radiotherapy, with at least one follow-up MRI performed post-radiotherapy (at intervals of 6–24 months); (4) Age ≥18 years (covering the primary radiotherapy population), all having voluntarily signed an informed consent form after understanding the specific details of the study.

***Exclusion criteria*:** (1) Neurodegenerative diseases such as multiple sclerosis and Alzheimer's disease; (2) Recent history of stroke (<6 months); (3) Concurrent administration of neurotoxic chemotherapy (e.g., methotrexate); (4) History of prior brain surgery.

Radiotherapy procedures

All patients received intensity-modulated radiation therapy (IMRT) or three-dimensional conformal radiation therapy (3D-CRT). The radiotherapy planning system used was Eclipse V15.6 (Varian, USA), and the medical linear accelerator was TrueBeam (Varian, USA). The total radiation dose ranged from 60.0 to 78.0 Gy, with a single dose of 2.0 –2.2 Gy. The dose volume histogram parameters included V30 (the volume fraction of brain tissue receiving ≥30 Gy of radiation) and D_{max} (the maximum radiation dose to brain tissue).

Imaging procedures

The imaging equipment was a Siemens Prisma 3.0T magnetic resonance scanner (Siemens AG, Germany). The contrast agent used was gadolinium meglumine injection (Bayer AG, Germany,

[Downloaded from ijrr.com on 2026-11-23]

[DOI: 10.61186/ijrr.24.4.30]

concentration 469 mg/mL). Scanning sequences included T2-weighted imaging (T2WI) and FLAIR. Two senior radiologists performed blind image interpretation using the Fazekas scoring system to quantify white matter hyperintensity (WMH) burden, with a total score ranging from 0 to 6, where higher scores indicate more severe white matter damage. MRI images were acquired before radiotherapy and at 6 months and 12 months post-radiotherapy to compare changes in white matter signal intensity.

APOE genotype testing

For APOE genotype testing, 5 mL of fasting peripheral venous blood from the patient was collect. DNA extraction kit: Tiangen Blood Genome DNA Extraction Kit (China Tiangen Biochemical Technology Co., Ltd.). Testing instrument: ABI 7500 real-time fluorescent quantitative PCR instrument (Thermo Fisher Scientific, USA). Testing loci: rs429358 and rs7412 single nucleotide polymorphism sites. The fluorescent probe hybridization method was used to distinguish APOE alleles, with individuals carrying at least one ε4 allele being classified as APOE ε4 carriers. All experiments were strictly performed in accordance with the kit instructions.

Specifically, genomic DNA was extracted from 200 μL of peripheral blood leukocytes using the Tiangen Blood Genome DNA Extraction Kit (Cat. No. DP318-03, Tiangen Biochemical Technology Co., Ltd., Beijing, China) following the manufacturer's spin-column protocol, with an elution volume of 100 μL. DNA concentration and purity were assessed using a NanoDrop 2000 spectrophotometer (Thermo Fisher Scientific, Wilmington, DE, USA), with all samples achieving A260/A280 ratios between 1.8 and 2.0. Genotyping of the two APOE single nucleotide polymorphisms (SNPs), rs429358 (c.388T>C, p.Cys130Arg) and rs7412 (c.526C>T, p.Arg176Cys), was performed using the ABI 7500 real-time fluorescent quantitative PCR system (Thermo Fisher Scientific, Foster City, CA, USA) with TaqMan SNP Genotyping Assays (Assay IDs: C__3084793_20 for rs429358 and C__904973_10 for rs7412; Thermo Fisher Scientific). Each 10 μL PCR reaction contained 5 μL of 2× TaqMan Genotyping Master Mix, 0.25 μL of 40× SNP Genotyping Assay mix, 10 ng of genomic DNA, and nuclease-free water. Thermal cycling conditions were: initial denaturation at 95°C for 10 minutes, followed by 40 cycles of 95°C for 15 seconds and 60°C for 1 minute. Fluorescence signals were measured at the end of each 60°C annealing/ extension step. Genotype calling was performed using the 7500 Software v2.3 (Thermo Fisher Scientific) with auto-call algorithm, and all genotype clusters were manually verified. APOE alleles were determined by combining the two SNP results: ε2 (rs429358=T, rs7412=T), ε3 (rs429358=T, rs7412=C), and ε4 (rs429358=C, rs7412=C). Samples with ambiguous genotype calls (n=3) were re-tested, and 10% of samples were randomly selected for Sanger sequencing validation (BigDye Terminator v3.1 Cycle Sequencing Kit, Applied Biosystems; 3500xL Genetic Analyzer, Applied Biosystems), yielding 100% concordance.

White matter hyperintensity assessment (Fazekas Score)

Fazekas Score [10], an imaging grading system for the severity of white matter hyperintensity (WMH) lesions, primarily based on T2-weighted or FLAIR sequence findings on MRI was used. It provides a comprehensive assessment by quantifying the pathological features of paraventricular white matter (PVWM) and deep white matter (DWM). The scoring criteria consist of two core regions: -Paraventricular white matter (PVWM): -0 points: No abnormal signals; -1 point: Point-like or pencil-thin lesions (e.g., cap-like hyperintensity at lateral ventricular angles); -2 points: Smooth halo-like lesions surrounding the ventricles; -3 points: Irregular hyperintensity extending into deep white matter with rough margins. -Deep white matter (DWM): -0 points: No lesions; -1 point: Scattered point-like lesions (mostly <5 mm in diameter); -2 points: Partial lesion fusion into plaque-like patterns (with early fusion tendency); -3 points: Extensive confluent lesions covering large white matter areas. The total score is the sum of PVWM and DWM scores (range: 0–6), corresponding to lesion severity: 1–2 points = mild, 3–4 points = moderate, 5–6 points = severe.

Dosimetric parameters (Dose-Volume Histogram)

Dosage-volume histogram parameters were derived from the three-dimensional dose distribution data in the radiotherapy planning system through quantitative analysis of the dose-volume relationship within specific anatomical structures (e.g., target volumes or critical organs). The patient's CT/MRI images are reconstructed into a three-dimensional voxel grid, where the absorbed dose value of each voxel (typically 1–3 mm^3) is calculated using the Monte Carlo algorithm or pencil-beam algorithm to generate a dose distribution matrix. Using image segmentation techniques, the contours of target volumes and critical organs are delineated, and the anatomical structures are mapped onto the dose grid. The dose values of all voxels within each structure are then statistically analyzed.

Diagnostic criteria for radiation encephalopathy

Diagnostic criteria for radiation encephalopathy [19]: Patients must have a clear history of head or whole-body radiotherapy, particularly with an annual dose ≥0.25 Gy and a cumulative whole-body dose ≥1.5 Gy; clinical manifestations are classified by disease course into the acute phase (days to weeks

[Downloaded from ijrr.com on 2026-11-23]

[DOI: 10.61186/ijrr.24.4.30]

post-radiotherapy, characterized primarily by acute intracranial hypertension symptoms such as headache, nausea, vomiting, and impaired consciousness), early-to-latent phase (1–6 months post-radiotherapy, presenting with cognitive decline including memory impairment, lethargy, and emotional abnormalities), and late-to-latent phase (6 months to years post-radiotherapy, manifesting irreversible neurological damage such as dementia, epilepsy, motor dysfunction, or brainstem/cerebellar deficits like ataxia and diplopia); typical imaging findings include hyperintensity in white matter (particularly bilateral frontal lobes), cerebral edema, or necrotic lesions; the Fazekas score can quantify the severity of white matter lesions; tumor recurrence, metastases, cerebrovascular diseases, or other organic brain pathologies must also be excluded.

Statistical methods

The data were analyzed using SPSS 25.0 statistical software (IBM, USA). Categorical data were analyzed using the χ^2 test; continuous variables were analyzed using the independent samples t-test; multivariate risk factors were analyzed using logistic regression; the predictive efficacy was evaluated using the ROC curve, with $P<0.05$ considered statistically significant.

RESULTS

Univariate analysis of factors influencing the risk of radiological encephalopathy

The RE group exhibited higher rates of APOE ε4 carriage, radiotherapy doses, Fazekas scores, V30 values, and Dmax values compared to the non-RE group, with statistically significant differences ($P<0.05$) (table 1).

Specifically, the APOE ε4 carrier rate was significantly higher in the RE group (70.59%, 12/17) compared to the non-RE group (37.50%, 51/136), with a statistically significant difference ($\chi^2 = 6.830$, $P=0.009$). The mean total radiotherapy dose was 75.36 ± 5.47 Gy in the RE group versus 67.25 ± 2.18 Gy in the non-RE group ($t = 11.574$, $P<0.001$). The mean Fazekas score was 2.47 ± 0.25 in the RE group and 1.84 ± 0.18 in the non-RE group ($t = 12.982$, $P<0.001$). The V30 value was 17.05 ± 2.04% in the RE group compared to 13.07 ± 1.77% in the non-RE group ($t = 8.593$, $P<0.001$). The Dmax was 73.25 ± 2.14 Gy in the RE group and 69.57 ± 2.36 Gy in the non-RE group ($t = 6.119$, $P<0.001$). No statistically significant differences were observed in age (RE: 52.3 ± 8.7 years vs. non-RE: 50.8 ± 9.2 years, $P=0.512$), sex distribution (male: 64.7% vs. 58.1%, $P=0.603$), or tumor type between the two groups.

Table 1. Univariate analysis of factors influencing the risk of radiation encephalopathy (RE). Data are presented as mean ± standard deviation for continuous variables or n (%) for categorical variables. RE: radiation encephalopathy; APOE: apolipoprotein E; V30: percentage of brain volume receiving ≥30 Gy; Dmax: maximum radiation dose to brain tissue; Gy: gray; χ^2: chi-square test statistic; t: independent samples t-test statistic; P: probability value.

Influencing factor		RE group (n=17)	Non-RE group (n=136)	t/χ^2	P
APOE ε4 carriers (n)	yes	12(70.59)	51(37.50)	6.830	0.009
	deny	5(29.41)	85(62.50)		
Radiotherapy dose (Gy)		75.36±5.47	67.25±2.18	11.574	<0.001
Fazekas score (points)		2.47±0.25	1.84±0.18	12.982	<0.001
V_{30} (%)		17.05±2.04	13.07±1.77	8.593	<0.001
D_{max} (Gy)		73.25±2.14	69.57±2.36	6.119	<0.001

Multivariate logistic regression analysis of factors influencing the risk of radiological encephalopathy

The occurrence of radiation brain syndrome was treated as the dependent variable (occurrence = 1, absence = 0), with APOE ε4 carriers, radiotherapy dose, Fazekas score, V_{30}, and D_{max} levels as independent variables. A multivariate logistic regression model was employed for quantitative analysis (table 2), revealing that APOE ε4 carriers, radiotherapy dose, Fazekas score, V30, and Dmax levels were significant risk factors for radiation brain syndrome ($P<0.05$; table 3).

Table 2. Quantitative assignment table.

variable	Value Description
Radiotherapy dose	continuous variable
APOE ε4 carrier	Yes = 1, No = 0
Fazekas score	continuous variable
V_{30}	continuous variable
D_{max}	continuous variable
Prevalence of radiological encephalopathy	Occurred = 1, Not occurred = 0

Table 3. Multivariate logistic regression analysis of independent risk factors for radiation encephalopathy (RE). The dependent variable was the occurrence of RE (1 = occurred, 0 = not occurred). β: regression coefficient; SE: standard error; Wald: Wald chi-square statistic; P: probability value; OR: odds ratio; 95% CI: 95% confidence interval; APOE: apolipoprotein E; V30: percentage of brain volume receiving ≥30 Gy; Dmax: maximum radiation dose to brain tissue; Gy: Gray.

factor	β	standard error	$Wald/\chi^2$	P	OR	95% confidence interval
Radiotherapy dose	1.132	0.193	34.405	<0.001	3.102	2.125~4.528
APOE ε4 carrier	0.827	0.075	121.363	<0.001	2.287	1.974~2.649
Fazekas score	1.437	0.191	56.554	<0.001	4.209	2.894~6.122
V_{30}	0.612	0.167	13.391	<0.001	1.845	1.329~2.561
D_{max}	0.913	0.174	27.457	<0.001	2.492	1.771~3.507

[Downloaded from ijrr.com on 2026-11-23]

[DOI: 10.61186/ijrr.24.4.30]

White matter changes before and after radiotherapy

MRI examinations were performed at three time points: before radiotherapy (baseline), 6 months post-radiotherapy, and 12 months post-radiotherapy. In the RE group, the mean Fazekas score increased progressively from 1.76 ± 0.32 at baseline to 2.12 ± 0.28 at 6 months (P<0.001 vs. baseline) and 2.47 ± 0.25 at 12 months (P<0.001 vs. 6 months). In the non-RE group, the Fazekas score showed a milder increase from 1.52 ± 0.29 at baseline to 1.68 ± 0.22 at 6 months (P=0.012 vs. baseline) and 1.84 ± 0.18 at 12 months (P=0.003 vs. 6 months). The between-group difference in Fazekas score change from baseline to 12 months was statistically significant (ΔFazekas: RE 0.71 ± 0.19 vs. non-RE 0.32 ± 0.15, t = 9.876, P<0.001). Regarding WMH lesion distribution, the proportion of patients with paraventricular white matter (PVWM) score ≥2 increased from 23.5% (4/17) at baseline to 70.6% (12/17) at 12 months in the RE group, compared to an increase from 14.0% (19/136) to 27.9% (38/136) in the non-RE group (χ^2 = 13.245, P<0.001). Deep white matter (DWM) score ≥2 was observed in 17.6% (3/17) of RE patients at baseline and 52.9% (9/17) at 12 months, versus 8.8% (12/136) and 16.2% (22/136) in the non-RE group (χ^2 = 11.567, P = 0.001). New-onset or enlarging white matter hyperintensities in the bilateral frontal lobes and periventricular regions were the most common imaging findings in the RE group at 12 months post-radiotherapy. Representative MRI FLAIR sequence images demonstrating varying levels of white matter changes is shown in figure 1.

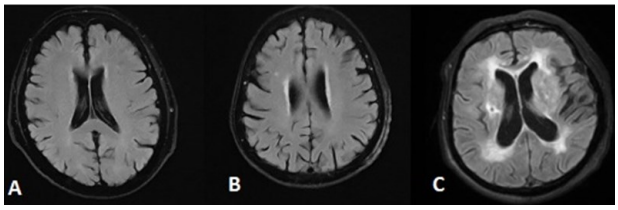


Figure 1. Representative MRI FLAIR sequence images demonstrating varying levels of white matter hyperintensity (WMH) signal intensity. **(A)** Low WMH burden (Fazekas score 0-1): Minimal punctate hyperintensities in the periventricular white matter, with no confluent lesions. This pattern was observed in 68.4% of the non-RE group at baseline. **(B)** Moderate WMH burden (Fazekas score 2-3): Smooth halo-like hyperintensity surrounding the lateral ventricles with early extension into deep white matter, and scattered punctate lesions in the deep white matter. This pattern was predominantly seen in patients who subsequently developed mild RE. **(C)** High WMH burden (Fazekas score 4-6): Extensive confluent hyperintensities in both periventricular and deep white matter regions, with irregular margins extending into the subcortical white matter. This pattern was observed in 76.5% of the RE group at 12 months post-radiotherapy. All images are axial FLAIR sequences (TR = 9000 ms, TE = 89 ms, TI = 2500 ms) acquired on a Siemens Prisma 3.0T scanner. White arrows indicate representative WMH lesions. RE: radiation encephalopathy; FLAIR: fluid-attenuated inversion recovery; TR: repetition time; TE: echo time; TI: inversion time.

ROC analysis of the risk of radiological encephalopathy

Based on the independent and dependent variables, the logistic regression analysis equation was established as follows: Logit(P) = β_0 + 1.132 × radiotherapy dose + 0.827 × APOE ε4 carrier (1 = yes, 0 = no) + 1.437 × Fazekas score + 0.612 × V30 + 0.913 × Dmax. The intercept (β_0) and predictor scaling must be checked against the original SPSS output before the equation is used for prediction.

ROC curve analysis revealed that the AUC values for predicting the occurrence of radiation-induced brain syndrome were 0.804 for radiotherapy dose, 0.885 for Dmax, 0.804 for the Fazekas score, and 0.850 for V30. The combined predictor demonstrated the highest AUC value (0.921), with all differences being statistically significant (P<0.05). The reported combined-predictor cutoff was 153.738 (table 4, figure 2); its calculation and clinical interpretation require confirmation against the original ROC output.

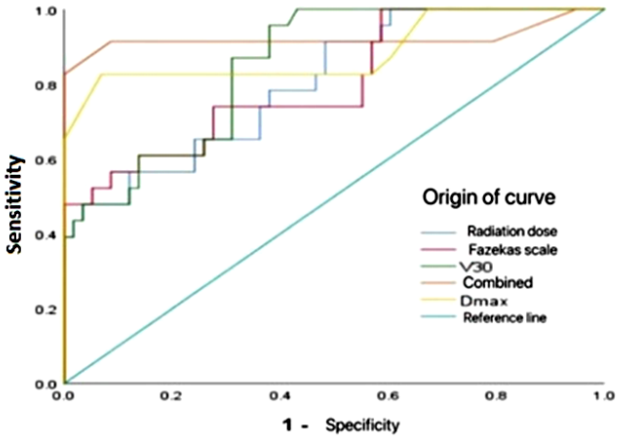


Figure 2. Receiver operating characteristic (ROC) curves for predicting radiation encephalopathy. The blue curve represents the combined prediction model (AUC = 0.921), for which the exact included predictors require verification against the original ROC analysis. The green curve represents Dmax alone (AUC = 0.885), the orange curve represents V30 alone (AUC = 0.850), the red curve represents radiotherapy dose alone (AUC = 0.804), and the purple curve represents Fazekas score alone (AUC = 0.804). The diagonal dashed line represents the reference line of no discrimination (AUC = 0.5). AUC: area under the curve; V30: percentage of brain volume receiving ≥30 Gy; Dmax: maximum radiation dose.

[Downloaded from ijrr.com on 2026-11-23]

[DOI: 10.61186/ijrr.24.4.30]

Table 4. Receiver operating characteristic (ROC) curve analysis for predicting radiation encephalopathy (RE). AUC: area under the curve; SE: standard error; 95% CI: 95% confidence interval; V30: percentage of brain volume receiving ≥30 Gy; Dmax: maximum radiation dose to brain tissue; Gy: gray; Combined: reported combined prediction model (included predictors require confirmation against the original ROC analysis).

metric	area under curve	standard error	*P*	95% confidence interval	Optimal cutoff value	sensitivity	specificity
Radiotherapy dose	0.804	0.051	<0.001	0.735~0.909	>70.125Gy	0.967	0.813
D_{max}	0.885	0.059	0.001	0.786~0.985	>72.590Gy	0.933	0.678
Fazekas score	0.804	0.019	<0.001	0.767~0.841	>2.530 points	0.733	0.578
V_{30}	0.850	0.038	<0.001	0.817~0.968	>16.020%	0.933	0.867
unite	0.921	0.051	<0.001	0.820~1.000	>153.738	0.733	0.578

DISCUSSION

Radiation brain syndrome, one of the most severe complications following radiotherapy for head and neck tumors, has long posed challenges for clinical decision-making due to its insidious progression and irreversible neurological damage [20]. Traditional diagnosis relies on delayed symptoms or late-stage imaging findings, by which time the therapeutic window has closed [21]. With the integration of neuroimagingomics and artificial intelligence, white matter hyperintensity (WMH) - a biomarker of early microvascular injury—is emerging as a novel key to addressing the challenge of predicting radiation brain syndrome. Related MRI-based research has used enhanced imaging features to predict short-term radiotherapy response in nasopharyngeal carcinoma, a different endpoint from radiation encephalopathy [22].

This study demonstrates that APOE ε4 carriers, radiation dose, Fazekas score, V30, and Dmax levels are influencing factors for the occurrence of radiation -induced encephalopathy post-radiotherapy. The underlying mechanisms are analyzed as follows: ① APOE ε4 carriers: The structural characteristics of the APOE ε4 protein result in functional defects. Compared to neutral APOE ε3, the ε4 variant exhibits poorer stability and is more prone to domain dissociation, leading to the formation of neurotoxic fragments. These fragments not only directly damage neurons but also abnormally bind to β-amyloid (Aβ), accelerating pathological deposition [23]. Under radiotherapy conditions, ionizing radiation itself induces oxidative stress and increased Aβ deposition, while the presence of ε4 further amplifies this pathological process, creating a vicious cycle of "radiation-Aβ-neuroinflammation" [24]. Additionally, as APOE serves as the primary cholesterol transporter in the brain, its ε4 subtype binds to neuronal sortilin receptors, impairing receptor recitation to the cell surface and disrupting lipid delivery pathways. This results in insufficient uptake of essential polyunsaturated fatty acids by neurons, reduced membrane stability, and decreased endogenous cannabinoid synthesis, thereby suppressing neuroinflammation and protecting synaptic function [25]. Due to impaired lipid transport, ε4 carriers exhibit significantly limited white matter repair capacity, manifesting as aggravated demyelination lesions post-radiotherapy [26]. Kim *et al*. [27] reviewed mechanisms of radiation-induced brain toxicity, including vascular injury and delayed neurological damage. ② Radiotherapy dose: When radiation penetrates brain tissue, high-dose radiation directly damages neuronal DNA structure, triggering irreversible apoptosis [27]. Concurrently, dose-dependent damage affects the cerebral microvascular system, leading to vascular endothelial cell death, basement membrane thickening, and luminal stenosis, ultimately resulting in ischemic necrosis of white matter. Higher doses cause more extensive vascular injury, exacerbating cerebral hypoxia and nutritional impairment, and ultimately forming necrotic foci [28]. Experimental animal-model evidence has also demonstrated oxidative damage and increased inflammatory markers after brain irradiation [29]. Additionally, high-dose radiotherapy rapidly damages vascular endothelial tight junction proteins, increasing blood-brain barrier permeability and allowing plasma proteins and inflammatory factors to infiltrate the brain parenchyma, inducing vascular-induced cerebral edema and neuroinflammatory cascade reactions. Such damage manifests as headache and nausea in the acute phase and progresses to delayed cerebral necrosis in the long term [30]. ③ Fazekas score: The Fazekas score (0 –6 points) assessed by MRI reflects the degree of ischemic injury in paraventricular and deep white matter. High scores (e.g., ≥Grade 2) indicate extensive microvascular pathology, compromising white matter microstructural integrity, impairing blood-brain barrier function, and reducing neural repair capacity [31]. When such patients undergo head and neck radiotherapy, radiation exerts a synergistic damaging effect on pre-existing vascular lesions: On one hand, radiotherapy-induced oxidative stress and inflammatory responses (e.g., release of TNF-α and IL -6) further compromise the already fragile microvascular endothelium, accelerating the breakdown of the blood-brain barrier; on the other hand, white matter demyelinating foci exhibit abnormal sensitivity to radiation, with radiotherapy directly inducing axonal degeneration and glial cell apoptosis in these areas, and the extent of damage increases exponentially with elevated Fazekas scores [32]. This "double-hit" mechanism predisposes high-

[Downloaded from ijrr.com on 2026-11-23]

[DOI: 10.61186/ijrr.24.4.30]

risk patients to radiation necrosis, manifesting as typical symptoms of radiation brain disease such as cognitive impairment and gait instability. Additionally, a high-risk status indicates depletion of antioxidant reserves in brain tissue (e.g., reduced superoxide dismutase activity), impairing the ability to eliminate radiotherapy-generated free radicals. Thus, higher Fazekas scores correspond to lower biological thresholds for irreversible white matter necrosis post-radiotherapy, ultimately serving as independent predictors of radiation brain disease [33]. ④ V_{30} and D_{max} levels: V_{30} quantifies the cumulative exposure range of moderate radiation doses (30 Gy). Elevated values indicate that a substantial volume of white matter receives radiation energy sufficient to damage the blood-brain barrier, triggering vascular endothelial injury and astrocyte activation, which leads to chronic inflammatory cascades. Clinically, this manifests as aggravated white matter hyperintensity (WMH) and eventual neurological dysfunction indicative of radiation brain disease [34]. Dmax focuses on the biological effects at the local maximum dose point. When the Dmax in critical brain regions (such as the brainstem and hippocampus) exceeds the tolerance threshold, it directly induces double-strand breaks in neuronal DNA and mitochondrial dysfunction, leading to acute necrosis or delayed coagulative necrosis. Particularly in high metabolic regions, radiation-induced oxidative stress further amplifies free radical damage, exceeding cellular repair capacity and resulting in irreversible necrotic foci [35]. When these two factors interact synergistically, V30 expands the extent of injury, while Dmax determines the depth of injury. Thus, V30 and Dmax precisely characterize the radiation exposure pattern in brain tissue through their physical dose distribution characteristics; exceeding these thresholds is directly associated with blood-brain barrier disruption, neuronal inflammation exacerbation, and irreversible damage to critical structures, constituting the core pathological basis of radiation-induced brain disease [36].

The radiotherapy dose, Dmax, Fazekas score, and V30 demonstrate significant value in predicting the occurrence of radiation-induced brain injury (RIBI). These four parameters- radiotherapy dose, Dmax, Fazekas score, and V30-cover the core pathological mechanisms of RIBI across four dimensions: radiation energy intensity, spatial distribution, brain tissue vulnerability, and cumulative dose effects. The radiotherapy dose and Dmax directly determine the extent of neuronal DNA damage and oxidative stress; high doses can induce irreversible vascular endothelial cell apoptosis and blood-brain barrier disruption. V30 quantifies the cumulative extent of subclinical damage, while high-dose, volumetric irradiation activates persistent inflammatory cascades that promote white matter demyelination. The Fazekas score assesses baseline white matter hyperintensity (WMH) burden, reflecting the severity of pre-existing cerebrovascular lesions; a high score (≥3) indicates diminished microcirculatory reserve function in brain tissue and a markedly reduced tolerance threshold for radiation injury [37]. These parameters exhibit a synergistic amplification effect: patients with high Fazekas scores exhibit inadequate white matter repair capacity even under moderate irradiation, accelerating radiation-induced necrosis; conversely, high D_{max} combined with extensive V_{30} irradiation can exceed the compensatory limits of patients with low Fazekas scores. This multidimensional interaction makes them indispensable indicators for RIBI risk prediction [38].

Taken together, these mechanistic insights are consistent with recent studies demonstrating that radiation-induced white matter injury involves a complex interplay between direct neuronal damage, microvascular injury, neuroinflammation, and impaired repair capacity [39, 40]. A longitudinal study by Liang *et al*. using multishell diffusion MRI identified radiation-associated white matter microstructural changes in patients with nasopharyngeal carcinoma and associations between diffusion measures and radiation dose [41]. Furthermore, a systematic review and meta-analysis by Dong et al. identified Dmax and D1cc as important dosimetric predictors of radiation-induced temporal lobe necrosis [42]. The integration of these dosimetric parameters with biological susceptibility markers (APOE ε4) and pre-existing imaging pathology (Fazekas score) in the present study represents a significant advance toward personalized risk assessment.

Furthermore, this study still has the following limitations: ① It is a single-center retrospective study with a limited sample size, which may introduce selection bias; ② Only the visual Fazekas score was employed, without utilizing artificial intelligence to quantify WMH volume; ③ The follow-up period was relatively short, lacking long-term neurological injury data beyond five years; ④ The molecular pathways through which APOE ε4 regulates radiation-induced brain injury were not thoroughly investigated. Subsequent research should include multicenter, prospective cohort studies combined with molecular experiments to refine mechanistic analyses. Therefore, the research team should conduct multicenter, large-sample, prospective randomized controlled trials to further deepen the analysis and provide more detailed and reliable evidence for improving the prevention and treatment of radiation-induced brain injury following radiotherapy.

[Downloaded from ijrr.com on 2026-11-23]

[DOI: 10.61186/ijrr.24.4.30]

CONCLUSION

In conclusion, MRI-based WMH burden, APOE ε4 gene subtype, and radiotherapy dosimetry parameters are independent risk factors for radiation encephalopathy. The multi-index combined predictive model demonstrates high accuracy and strong operability, enabling early identification of RE risk in patients receiving radiotherapy for head and neck tumors. It provides an objective reference for developing personalized clinical radiotherapy protocols and implementing follow-up interventions for high-risk populations.

Acknowledgments: The authors thank all patients and their families for their participation in this study. We gratefully acknowledge the Department of Radiology and the Department of Radiation Oncology for their assistance with image acquisition and data collection. We also thank the medical physics team for their support in dosimetric data extraction.

Funding: This work was supported by the National Natural Science Foundation of China [Grant No. 82272091] and the Provincial Key Research and Development Program [Grant No. 2023-SF-145]. The funding bodies had no role in the study design, data collection, analysis, interpretation, or writing of the manuscript.

Ethical consideration: This study was approved by the Medical Ethics Committee of The Affiliated Hospital [Approval No.: KY-2025-0612; Approval Date: June 8, 2025]. All procedures performed in studies involving human participants were in accordance with the ethical standards of the institutional research committee and with the 1964 Helsinki Declaration and its later amendments or comparable ethical standards. Written informed consent was obtained from all individual participants included in the study.

Conflict of interest: The authors declare that they have no known competing financial interests or personal relationships that could have appeared to influence the work reported in this paper.

Authors' contribution: H.G.: Conceptualization, methodology, investigation, data curation, writing - original draft, writing - review & editing, supervision, project administration, funding acquisition. G.T.: Software, formal analysis, data curation, writing - review & editing, visualization. Y.Z.: Investigation, resources, data curation, writing - review & editing. All authors have read and agreed to the published version of the manuscript.

AI usage statement: During the preparation of this manuscript, the authors used artificial intelligence (AI) tools specifically for English language grammar polishing and formatting assistance. The AI tool was used solely to improve the clarity and readability of the English text. All experimental data, analytical results, scientific interpretations, and research conclusions were independently generated and verified by the authors. No AI-generated content was included without thorough human review and validation. The authors take full responsibility for the accuracy and integrity of all content in this manuscript.

REFERENCES

1. Li Z, Zhan Z, Lai Y (2022) Radiation optic neuropathy diagnosis in nasopharyngeal carcinoma patients with radiation encephalopathy. *Eur J Ophthalmol*, ***32***(6): 3657–3666.
2. Qin CH, Qiu SJ, Wang HZ, Duan FH, Wu DL, Leng X (2022) A Study on the correlation between brain functional and structural changes and altered cognitive function after radiotherapy for nasopharyngeal carcinoma. *Int J Radiat Res*, ***20***(3): 627–633.
3. Soussain C, Ricard D, Fike JR, Mazeron JJ, Psimaras D, Delattre JY (2009) CNS complications of radiotherapy and chemotherapy. *Lancet*, ***374***(9701): 1639–1651.
4. Greene-Schloesser D, Robbins ME, Peiffer AM, Shaw EG, Wheeler KT, Chan MD (2012) Radiation-induced brain injury: A review. *Front Oncol*, ***2***: 73.
5. Bell RD, Winkler EA, Singh I, Sagare AP, Deane R, Wu Z, *et al.* (2012) Apolipoprotein E controls cerebrovascular integrity via cyclophilin A. *Nature*, ***485***(7399): 512–516.
6. Wang J, Miao Y, Ou X (2019) Development and validation of a model for temporal lobe necrosis for nasopharyngeal carcinoma patients with intensity modulated radiation therapy. *Radiat Oncol*, ***14***(1): 42.
7. Zhou X, Liu P, Wang X (2021) Temporal lobe necrosis following radiotherapy in nasopharyngeal carcinoma: New insight into the management. *Front Oncol*, ***10***: 593487.
8. Zhou GQ, Yu XL, Chen M, Guo R, Lei Y, Sun Y, *et al.* (2013) Radiation-induced temporal lobe injury for nasopharyngeal carcinoma: a comparison of intensity-modulated radiotherapy and conventional two-dimensional radiotherapy. *PLoS One*, ***8***(7): e67488.
9. Hsiao KY, Yeh SA, Chang CC, Tsai PC, Wu JM, Gau JS (2010) Cognitive function before and after intensity-modulated radiation therapy in patients with nasopharyngeal carcinoma: a prospective study. *Int J Radiat Oncol Biol Phys*, ***77***(3): 722–726.
10. Fazekas F, Chawluk JB, Alavi A, Hurtig HI, Zimmerman RA (1987) MR signal abnormalities at 1.5 T in Alzheimer's dementia and normal aging. *AJR Am J Roentgenol*, ***149***(2): 351–356.
11. Qiu Y, Guo Z, Lin X (2021) Standard radiotherapy for patients with nasopharyngeal carcinoma results in progressive tract-specific brain white matter alterations: A one-year follow-up via diffusion tensor imaging. *Radiother Oncol*, ***159***: 255–264.
12. Lin X, Tang L, Li M (2021) Irradiation-related longitudinal white matter atrophy underlies cognitive impairment in patients with nasopharyngeal carcinoma. *Brain Imaging Behav*, ***15***(5): 2426–2435.
13. Corder EH, Saunders AM, Strittmatter WJ, Schmechel DE, Gaskell PC, Small GW, *et al.* (1993) Gene dose of apolipoprotein E type 4 allele and the risk of Alzheimer's disease in late onset families. *Science*, ***261***(5123): 921–923.
14. Li L, Bao Y, He S (2015) The association between apolipoprotein E and functional outcome after traumatic brain injury: A meta-analysis. *Medicine (Baltimore)*, ***94***(46): e2028.
15. Villasana L, Acevedo S, Poage C (2006) Sex- and APOE isoform-dependent effects of radiation on cognitive function. *Radiat Res*, ***166***(6): 883–891.
16. Villasana L, Dayger C, Raber J (2013) Dose- and ApoE isoform-dependent cognitive injury after cranial 56Fe irradiation in female mice. *Radiat Res*, ***179***(4): 493–500.
17. Su SF, Huang SM, Han F, Huang Y, Chen CY, Xiao WW, *et al.* (2013) Analysis of dosimetric factors associated with temporal lobe necrosis (TLN) in patients with nasopharyngeal carcinoma (NPC) after intensity modulated radiotherapy. *Radiat Oncol*, ***8***: 17.
18. Pan J, Liang J, Li Y (2025) Composite quantitative structural magnetic resonance imaging-based risk scoring model for predicting radiation-induced temporal lobe necrosis in nasopharyngeal carcinoma: a novel risk stratification model. *Radiat Oncol*, ***20***(1): 160.
19. Lee AW, Ng SH, Ho JH, Tse VK, Poon YF, Tse CC, *et al.* (1988) Clinical diagnosis of late temporal lobe necrosis following radiation therapy

[Downloaded from ijrr.com on 2026-11-23]

[DOI: 10.61186/ijrr.24.4.30]

for nasopharyngeal carcinoma. *Cancer*, **61**(8): 1535–1542.
20. Zhang Y, Ou G, Li Q (2022) Treatment strategies for radiation-induced brain injury. *Int J Radiat Res*, **20**(4): 727–736.
21. Iyizoba-Ebozue Z, Prestwich R, Brown S (2023) Neurocognitive function following (chemo)radiotherapy for nasopharyngeal cancer and other head and neck cancers: A systematic review. *Radiother Oncol*, **188**: 109863.
22. Liu X, Pang H, Zhou H (2025) The value of imaging techniques based on enhanced magnetic resonance imaging in the diagnosis and prediction response of radiotherapy for nasopharyngeal carcinoma. *Int J Radiat Res*, **23**(2): 311–316.
23. Liu CC, Kanekiyo T, Xu H, Bu G (2013) Apolipoprotein E and Alzheimer disease: risk, mechanisms and therapy. *Nat Rev Neurol*, **9**(2): 106–118.
24. Monje ML, Mizumatsu S, Fike JR, Palmer TD (2002) Irradiation induces neural precursor-cell dysfunction. *Nat Med*, **8**(9): 955–962.
25. Montagne A, Nation DA, Sagare AP, Barisano G, Sweeney MD, Chakhoyan A, *et al.* (2020) APOE4 leads to blood-brain barrier dysfunction predicting cognitive decline. *Nature*, **581**(7806): 71–76.
26. Blanchard JW, Akay LA, Davila-Velderrain J, Maydell D von, Mathys H, Davidson SM, *et al.* (2022) APOE4 impairs myelination via cholesterol dysregulation in oligodendrocytes. *Nature*, **611**(7937): 769–779.
27. Kim JH, Brown SL, Jenrow KA, Ryu S (2008) Mechanisms of radiation-induced brain toxicity and implications for future clinical trials. *J Neurooncol*, **87**(3): 279–286.
28. Kim JH, Jenrow KA, Brown SL (2014) Mechanisms of radiation-induced normal tissue toxicity and implications for future clinical trials. *Radiat Oncol J*, **32**(3): 103–115.
29. Sever IH, Ozkul B, Atasoy O, Cini N, Bozkurt MF, Erdogan MA, *et al.* (2023) Neuroprotective effect of polyethylene Glycol (PEG-3350) on radiation-induced brain injury via membrane stabilization. *Int J Radiat Res*, **21**(4): 733–743.
30. Ye J, Rong X, Xiang Y (2012) A study of radiation-induced cerebral vascular injury in nasopharyngeal carcinoma patients with radiation-induced temporal lobe necrosis. *PLoS One*, **7**(8): e42890.
31. Wardlaw JM, Smith EE, Biessels GJ, Cordonnier C, Fazekas F, Frayne R, *et al.* (2013) Neuroimaging standards for research into small vessel disease and its contribution to ageing and neurodegeneration. *Lancet Neurol*, **12**(8): 822–838.
32. Pantoni L (2010) Cerebral small vessel disease: from pathogenesis and clinical characteristics to therapeutic challenges. *Lancet Neurol*, **9**(7): 689–701.
33. Debette S and Markus HS (2010) The clinical importance of white matter hyperintensities on brain magnetic resonance imaging: systematic review and meta-analysis. *BMJ*, **341**: c3666.
34. Zhou X, Ou X, Xu T (2014) Effect of dosimetric factors on occurrence and volume of temporal lobe necrosis following intensity modulated radiation therapy for nasopharyngeal carcinoma: a case-control study. *Int J Radiat Oncol Biol Phys*, **90**(2): 261–269.
35. Kong C, Zhu XZ, Lee TF, Feng PB, Xu JH, Qian PD, *et al.* (2016) LASSO-based NTCP model for radiation-induced temporal lobe injury developing after intensity-modulated radiotherapy of nasopharyngeal carcinoma. *Sci Rep*, **6**: 26378.
36. Lawrence YR, Li XA, Naqa IEl, Hahn CA, Marks LB, Merchant TE, *et al.* (2010) Radiation dose-volume effects in the brain. *Int J Radiat Oncol Biol Phys*, **76**(3 Suppl): S20–S27.
37. Prins ND, Dijk EJ van, Heijer T den, Vermeer SE, Koudstaal PJ, Oudkerk M, *et al.* (2004) Cerebral white matter lesions and the risk of dementia. *Arch Neurol*, **61**(10): 1531–1534.
38. Makale MT, McDonald CR, Hattangadi-Gluth JA, Kesari S (2017) Mechanisms of radiotherapy-associated cognitive disability in patients with brain tumours. *Nat Rev Neurol*, **13**(1): 52–64.
39. Balentova S and Adamkov M (2015) Molecular, Cellular and Functional Effects of Radiation-Induced Brain Injury: A Review. *Int J Mol Sci*, **16**(11): 27796–27815.
40. Voon NS, Lau FN, Zakaria R, Md Rani SA, Ismail F, Manan HA, *et al.* (2021) MRI-based brain structural changes following radiotherapy of Nasopharyngeal Carcinoma: A systematic review. *Cancer Radiother*, **25**(1): 62–71.
41. Liang J, Zhang X, Lin Y (2024) Disparate Radiation-Induced Microstructural Injuries in Whole-Brain White Matter of Patients With Nasopharyngeal Carcinoma: A Longitudinal Study Using Multishell Diffusion MRI. *J Magn Reson Imaging*, **59**(3): 976–986.
42. Dong J, Ng WT, Wong CHL, Li JS, Bollen H, Chow JCH, *et al.* (2024) Dosimetric parameters predict radiation-induced temporal lobe necrosis in nasopharyngeal carcinoma patients: A systematic review and meta-analysis. *Radiother Oncol*, **195**: 110258.

[Downloaded from ijrr.com on 2026-11-23]

[DOI: 10.61186/ijrr.24.4.30]

[DOI: 10.61186/ijrr.24.4.30] [Downloaded from ijrr.com on 2026-11-23]